Common Envelope Evolution of Stars

Luke Chamandy, Adam Frank, Eric G. Blackman, Baowei Liu & Jonathan Carroll-Nellenback

Response to Reviewers' reports

As the original proposal was rejected, here we include a brief reply to the reviewers' reports.

Review 1

The proposal studies the common envelope (CE) phase of binary star evolution, which is a challenging problem. It is addressed by using AMR-MHD multi-physics code.

Methodology
The methodology is appropriate

Research plan
They use Stampede2. They have provided scaling tests but the proposal is unclear on the number of requested nodes

We have now provided this information in Sec. 3.3.

Review 2

The researchers appear to have made good use of their previous extension (resulting in 1 new paper).

Our XSEDE allocation contributed to a number of papers and conference proceedings in the past year, as mentioned now in the progress report.

The science case continues to be relevant. However, a critical problem with the proposed extension is that we were unable to understand the basis of estimate for the number of requested node-hours. While the proposers discuss the measured scaling on both SKX and KNL nodes, they don't show in a way that we were able to follow how those numbers translate into the numbers on node-hours listed in Table 2.

We have now directly calculated the node hours listed in the table (now Table 1) using the results of the scaling tests on SKX and KNL nodes. This is now laid out in Sections 3.3 and 5.

Secondly, they don't clearly specify whether those node-hours are for Skylake or KNL nodes, which makes for a substantial difference. We recommend these issues are addressed and proposal resubmitted at a later time.

We understand the reviewer's point. Normally we prefer the SKX nodes, but given that the demand on these nodes is high, to have the option to sometimes avoid long queue times we have requested to do 10% of our computation using KNL nodes. We now calculate the node-hours based on this

90-10 division in the number of simulation frames, by simple arithmetic from the scaling tests and total number of frames proposed.

A second issue is that the proposal is very detailed and too extensive (and repetitive in some areas – e.g., the same plots appear in the main body and in the discussion of scaling).

We have now removed the figures relating to scaling from the main document, and included them only in the code performance and scaling document. We have also streamlined the text. Finally, we have simplified the table of runs. We have removed the convergence tests but request 10% of the total requested allocation for convergence studies and test runs. We have added two new runs (Runs 14 and 15) that we expect will be useful. They involve jets in common envelope evolution with an asymptotic giant primary. Such systems are particularly promising for obtaining unbound envelopes and are directly relevant to the study of planetary nebulae.

We ask the authors to trim the text and strictly adhere to guidelines on the number of pages, margins, and allowed font size.

We are grateful to the reviewers for pointing out the guidelines, and we have now strictly adhered to them (e.g. we have stayed withing the 10 page limit not counting this response to the reviewer's comments).

Methodology
The methodology appears appropriate.

Research plan
The methodology appears appropriate.

Resource Use
KNL nodes show less efficient scaling (35% drop relative to ideal vs. 10% on SKX). It's also not clear whether the requested node-hours refer to KNL or SKX nodes (the difference isn't insignificant).

This has now been made clear in Sections 3.3 and 5.

1 Research Objectives

Common envelope evolution (CEE) is a strongly interacting phase of binary stellar evolution whose consequences are fundamental to understanding the end states of solar mass stars (planetary nebulae; PNe), the progenitors of supernovae type Ia, and the progenitors of compact binaries that become gravitational wave sources. CEE occurs when a binary orbit decays to the point that the secondary plunges into the envelope of the primary (Fig. 1: Paczynski 1976). Dissipative losses drive a fast inspiral of the secondary leading to the ejection of the envelope. CEE is thought to be the principal mechanism by which binary stars on very short orbits are created. After decades of study however, fundamental questions about CEE remain (Taam & Sandquist, 2000; Ivanova et al., 2013). For example, the link between initial states and final outcomes is unsettled, the precise mechanisms driving inspiral have not been studied in detail and which physical processes dominate remains uncertain. The challenge is exacerbated by the inherent 3-D multi-physics nature of CEE,

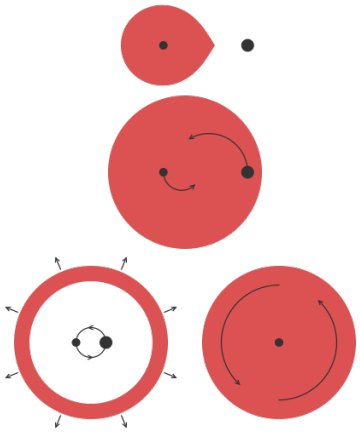

Figure 1: Schematic of common envelope evolution which occurs when a binary orbit decays to the point that the secondary plunges into the envelope of the primary, expelling the envelope leading to a tight binary or else merging with the giant's core.

Until recently there have been few numerical studies of the process and the majority of which have employed smooth particle hydrodynamic techniques (see Iaconi et al., 2017, for a comprehensive list of CE simulations from the literature). Only in the last few years have grid based codes (AMR in particular) tackled the problem. CEE is therefore a timely grand challenge problem for stellar astrophysics that has yet to incur the extensive numerical simulation effort supernova explosions or star formation have benefited from. CEE requires simulating a wide, dynamically coupled range of physical processes and scales. Recent advances in numerical modeling however, now allow the CEE problem to be more fully addressed. We propose to use our successful AMR MHD multi-physics CE code AstroBEAR to further propel the study of CEE physics and its consequences for evolved binary stars forward. Our proposed CEE work has the following interconnected objectives, outlined below.

1.1 Common Envelope Evolution with a Jet

The high accretion rates onto the secondary and the large specific angular momentum in the accretion flow, as demonstrated in Chamandy et al. (2018b), provide the circumstance for jets to form in such systems. Jets carry away kinetic energy as gas accretes deeper into the potential well of the secondary. This is distinct from kinetic energy released from the shrinking orbit as the secondary and primary core inspiral. Jets thus act as an extra source of energy input into the envelope. More energy transferred to the envelope can more rapidly unbind the envelope (Soker, 2017; Shiber & Soker, 2018), which in turn would also affect the final separation $a_{\rm f}$ between the secondary and primary core. Self-consistent jet formation would require magnetic fields and impractically high resolution, so incorporating a jet in a 3D global CEE simulation via an imposed subgrid model is the most practical approach. Our group has developed and tested a suitalble jet feedback subgrid model (Fogerty, 2017), similar to that of Federrath et al. (2014). It launches a bi-conical jet centered on the secondary point particle, parameterized by the accretion rate, which is set to a constant fraction of the Eddington rate for the companion, as in accretion disk theory. The jet will be activated as long as the mass inside the designated accretion zone is sufficient to provide the specified accretion rate.

To understand the implications of jet outcomes, we need to compare jets of different mechanical power, which in turn, is determined by accretion rate. Toward this end, we will study the consequences of varying the accretion rate over the range $\dot{M} \sim (0.1\text{–}100)\dot{M}_{\rm Edd}$. We will also study how deeply into the CE such a jet can operate. before thermalizing and quenching accretion.

1.2 Common Envelope Evolution in Triple Systems

About 10% of solar-like stars are in triple systems (Raghavan et al., 2010; Duchêne & Kraus, 2013). Systems with more than two components are observed to be preferentially younger, suggesting that they disrupt by long term dynamical interaction (Raghavan et al., 2010). The percentage of triple systems increases with mass (Duchêne & Kraus, 2013; De Marco & Izzard, 2017), and it is possible that the RGB star modeled in our simulations could be in a triple with a pair of binary white dwarfs that evolved from more massive progenitors. Many binary white dwarfs in close orbits of $\sim 1\,$d are known and studied (Gianninas et al., 2014). What effect would CEE have on the evolution of the orbits and envelope morphology in a triple system?

Planets orbiting the secondary provide another motivation to consider triple systems. Most stars are expected to have planets, some of which are 'hot Jupiters' orbiting with periods of order 1 d. Such objects have been found orbiting one stars of a binary system (Günther et al., 2018). Would the planet's orbit be disrupted by the CEE, and if so, how? In spite of the potential importance of triples, CEE of such mutiple stellar systems or binary+planet systems has not yet been explored.

1.3 Common Envelope Evolution with an Asymptotic Giant Branch Star

High resolution global 3D CEE simulations in the literature have so far been limited to binary systems involving a RGB primary, but studying systems involving AGB primaries is an essential next step. The AGB is a later stage in the evolution of a star compared with the RGB, and AGB stars are larger than their RGB counterparts, but have similar mass. The progenitors of planetary nebulae (PNe) and pre-planetary nebulae (PPNe) likely involve AGB stars rather than RGB stars (Balick & Frank, 2002) and binarity is needed to explain the bipolar symmetry and large collimated outflow momenta seen in many of these objects (**?**). The small separations of some binary PN central stars imply that these systems passed through a CE phase (Soker, 1994; Reyes-Ruiz & López, 1999; Nordhaus & Blackman, 2006; De Marco et al., 2013; Jones & Boffin, 2017). Most PNe and PPNe and most of the post-CE binaries observed probably result from a CE phase involving an AGB primary.

Due to its more distended structure, an AGB star is more loosely bound than its RGB progenitor so that a CE interaction is more likely to completely unbind (eject) the envelope. Further, if the envelope is ejected, this will occur at a larger final separation $a_{\rm f}$ of the giant core and secondary than for the case of a RGB primary. Applying the so-called CE energy formalism (Ivanova et al., 2013), the final separation is found to be ~ 4 times larger for the $2\,{\rm M}_\odot$ zero-age main sequence model explored, irrespective of the value of the efficiency parameter $\alpha_{\rm CE}$ (Chamandy et al., 2018a). This is important because the minimum separation attainable in simulations is limited by the resolution. CEE involving AGB stars overall more likely to unbind the envelope in simulations than RGB stars, even when taking into account the lower physical resolution implied by the larger system size (about a factor of 2 larger). RGB envelopes have only unbinded in simulations when recombination energy is included as an additional energy source (Nandez & Ivanova, 2016). However, recombination energy may be radiated away before it can be absorbed to contribute much to envelope ejection (Sabach et al., 2017; Grichener et al., 2018; Ivanova, 2018). Unbinding of the envelope is a key goal of CEE simulations because it would allow us to make contact with observed post CE binary

systems, such as the binary central stars of PNe. Studying CEE in AGB stars is the most promising way to achieve envelope unbinding given current numerical constraints.

Jets are as relevant for CEE involving AGB primaries as they are for RGB primaries. We intend to investigate the role of jets in AGB CEE simulations as well. By simulating jets in both RGB and AGB CEE simulations we will compare how jet propagation and quenching depend on the jet environment and evolutionary state of the primary star.

2 Computational Methods

2.1 AstroBEAR

AstroBEAR is an Adaptive Mesh Refinement (AMR), multi-physics code for astrophysics. AMR remains at the cutting edge of computational astrophysics. AstroBEAR uses a hierarchical approach to parallelization suitable for multicore architectures in which large-scale patches of data are distributed to nodes using MPI and the work for an individual patch is distributed across the cores on a node using OpenMP directives. AstroBEAR also employs new techniques such as load balancing by threading the grid advances on each level with preference going to the finer level grids.

The multi-physics capabilities of AstroBEAR have been significantly expanded by including solvers for elliptic and parabolic equations. Adapting the linear system solver HYPRE, we now routinely simulate systems in which self-gravity, heat conduction, magnetic resistivity and radiation transfer are important. In addition, AstroBEAR can treat gravitationally interacting point particles which accrete mass.

The UR astrophysics group successfully constructed and tested AstroBEAR, a fully parallelized, multi-dimensional AMR MHD code. The success of this effort is evidenced both in the code's completion (Cunningham et al., 2009) and the papers published using AstroBEAR as it was developed through its radiation-hydrodynamic and MHD versions (a partial list includes: Poludnenko et al. (2004); Cunningham et al. (2005, 2006, 2009); Yirak et al. (2012); Carroll-Nellenback et al. (2013); Huarte-Espinosa et al. (2013b,a); Li et al. (2014); Kaminski et al. (2014); Hansen et al. (2015a,b); Hartigan et al. (2016); Chen et al. (2016a,b); Fogerty et al. (2016)).

2.2 CEE Simulations with AstroBEAR

Our hydrodynamic simulations begin with a stable RGB or AGB primary star in a binary orbit with a main sequence or white dwarf secondary companion. Both the secondary and the core of the primary are modeled as gravitation-only point particles. We account self-consistently for all gravitational interactions (particle–particle, particle–gas, and gas–gas).

To set up the CEE initial conditions, we performed a 1D spherically symmetric simulation of the primary star using the stellar evolution code MESA (Paxton et al., 2011, 2013, 2015). The stellar profile was then modified to account for the coarser resolution of the 3D grid compared to the 1D grid. First, the core was replaced with a point particle and then the equations of stellar structure were solved using the new potential (Ohlmann et al., 2017; Chamandy et al., 2018b). This produces a stable RGB or AGB primary star. The much smaller secondary star, modeled as a point particle, is then added to the grid just above the surface of the RGB or AGB star, and the two stars are initialized in a circular orbit. The simulation frame is the center of mass frame.

2.3 Storage and Analysis

Simulation data is stored as hdf5 chombo files. Most of the analysis will be done using parallelized tools built into the AstroBEAR package that can be performed at run time or in post processing. We will also use our local visualization resources such as VisIt for analyzing the data. During analysis, data will be stored locally on the University of Rochester's BlueHive cluster. However, the data cannot be retained there permanently due to the high cost of storage rental. Therefore, data will be copied from Stampede 2 scratch to TACC Ranch for longer term storage.

3 Application Efficiencies

3.1 Scaling Tests

We performed strong scaling tests on KNL and SKX Stampede 2 at TACC, shown in Fig. 2 in the code performance and scaling document. These tests were done with our fiducial run (Model A of Chamandy et al. 2018b) at a resolution of 512^3 with 5 additional levels of AMR, for 1/10 of a frame. The number of cells refined at the highest AMR level decreased with time during the fiducial simulation, while the highest AMR level was increased from 4 to 5 about half way through the simulation. These two effects cancel somewhat so that the number of SUs required per frame is not drastically different at the beginning and end of the fiducial simulation. The frame we chose for the scaling runs is actually somewhat less demanding in SUs than the mean SU requirement per frame for that run. However, it will probably be fairly average for the proposed runs, which will be run for about 50% more frames, with the required SU per frame decreasing gradually with time since the highest AMR level will be kept constant at 5 during those extra frames.

For SKX nodes, the strong scaling shows a slope of -0.91 up to 128 nodes, and for KNL nodes, it shows a slope of -0.69 up to 256 nodes. (Perfect scaling corresponds to a slope of -1.) This demonstrates very good scaling of AstroBEAR on Stampede 2 for the simulations we seek to perform, especially for the SKX nodes. We also performed weak scaling tests shown in Fig. 3 of the code performance and scaling document. to study how the code performed when the workload per core was held constant at 512^2 zones. In general this helps to determine how the communication scales. Our weak scaling results show a drop in efficiency of 10% out to 128 SKX nodes and 35% out to 256 KNL nodes on Stampede 2.

3.2 Storage

The average chombo size will be comparable for all runs. The fiducial run of about 200 frames resulted in 10 TB of data, for an average chombo size of 50 GB per frame. The frame rate of 5 frames per simulation day is chosen to be the same for all runs.

3.3 Choice of Resources

As our code runs more efficiently on SKX nodes, we will use them to perform the majority of the computations. However, since these nodes are in high demand, we calculate the required node-hours assuming that 10% of the computations (i.e. 10% of the frames) will employ KNL nodes. We plan to perform the calculations using 64 SKX nodes or 128 KNL nodes. These numbers were chosen as a reasonable compromise between computational efficiency and wall time needed per frame. From the strong scaling detailed in the code performance and scaling document, using 64 SKX nodes, 1/10 of a frame was completed in about 200 s, which translates to 36 node-hours per frame. From the same figure, the corresponding time for 128 KNL nodes was about 500 s, which translates to

about 180 node-hours per frame. With 90% of the frames simulated using SKX nodes and the remaining 10% with KNL nodes, we obtain an average usage of about 50 node-hours per frame.

For our storage needs, we plan to store the data on TACC Ranch after it has been analyzed, in order to make space for new data on our local machines. Since frequent access to the data will not be needed at that stage, Ranch is a suitable storage solution.

4 Computational Research Plan

4.1 Common Envelope Evolution Involving a Jet

Tab. 1 contains the list of proposed runs. Runs 1 and 2 restart from frame 0 of the fiducial run of Chamandy et al. (2018b,a) but now include a jet around the secondary. They will end at $t = 20\,\mathrm{d}$ to allow us to see the jet progress dynamically from unquenched to quenched after it enters denser regions. In Runs 3-6, the simulation is restarted from $t = 20\,\mathrm{d}$, or halfway through the ~ 200 frame fiducial run. The latter two runs are designed to test high accretion rates of $\dot{M}/\dot{M}_{\mathrm{Edd}} = 10$ and 100 that are possible when the secondary is deep inside the envelope (Chamandy et al., 2018b).

We will also explore the dependence of jet activity on secondary mass. Since we have already performed a simulation identical to the fiducial run but with a secondary mass equal to $0.5\,\mathrm{M}_\odot$ instead of $1\,\mathrm{M}_\odot$, we will restart with a jet from snapshots of that simulation. Thus, in Runs 7 and 8, we repeat Runs 2 and 5 but now with a secondary of half the mass. To allow enough time for the jet to evolve, for example for the jet to be quenched, we plan to run all of these models for a duration of 20 d, or 100 frames.

4.2 Common Envelope Evolution in Triple Systems

We will perform four runs to study CEE triples. The extra computation required to evolve an additional point particle is minimal because the number of computations is dominated by the hydrodynamics and gas-gas gravitational interaction rather than the particle-gas or particle-particle gravitational interactions. Two point particles will be initialized in a small binary orbit, with their center of mass orbiting the RGB primary in the same initial circular orbit as in the fiducial model. Run 9, will involve secondary and tertiary components with a mutual separation of $6\,\mathrm{R}_\odot$, and with masses of $M_2 = M_3 = 0.5\,\mathrm{M}_\odot$. The combined mass of $1\,\mathrm{M}_\odot$ enables useful comparison with the fiducial binary run which had $M_2 = 1\,\mathrm{M}_\odot$. Run 10 will double the tertiary-secondary separation to explore its effect on the evolution. In Run 11 we will set the mass ratio to $M_2/M_3 = 2$ choosing choose $M_2 = \frac{2}{3}\,\mathrm{M}_\odot$ and $M_3 = \frac{1}{3}\,\mathrm{M}_\odot$ to keep the total mass the same. Finally, we will explore the fate of a hot Jupiter orbiting a $1\,\mathrm{M}_\odot$ secondary in Run 12 by putting $M_3 = 10^{-3}\,\mathrm{M}_\odot$. These simulations will be evolved for 60 d or 300 frames. This is about 50% longer than the fiducial binary run and about half as long as the binary CEE simulation of (Ohlmann et al., 2016).

4.3 Common Envelope Evolution Involving an AGB Primary

To study CEE involving an AGB star we will use a very similar setup to the fiducial model of Chamandy et al. (2018b), also used in Chamandy et al. (2018a), but now with the RGB primary replaced by an AGB primary. The AGB star profile is taken from a later stage of the same 1D stellar evolution simulation used to obtain the profile of the RGB star. As the AGB is about twice the size of the RGB the simulation domain will be scaled up by a factor of two, which means that the smallest resolution element is twice as large.

Table 1: Proposed simulation runs and projected node-hours assuming an average of 50 node-hours per frame using a combination of SKX and KNL nodes as detailed in Sec. 3.3. Quantities are: M_2: Mass of secondary; M_3: Mass of tertiary, if present; a_{2-3}: Separation between secondary and tertiary; $\dot{M}/\dot{M}_{\rm Edd}$: Accretion rate relative to Eddington value for a $0.01\,{\rm R}_\odot$ white dwarf, if a jet is present; *Restart frame*: Frame at which the simulation is restarted from the fiducial RGB simulation or the AGB simulation with no jet; *SUs*: Projected number of service units (node hours); *Data*: Projected storage requirement for simulation output.

		M_2 ($\rm M_\odot$)	M_3 ($\rm M_\odot$)	a_{2-3} ($\rm R_\odot$)	$\dot{M}/\dot{M}_{\rm Edd}$ ($\rm M_\odot$)	Restart frame	Number of frames	SUs	Data (TB)
1	RGB+Jet	1	–	–	0.1	0	100	5,000	5
2	RGB+Jet	1	–	–	1	0	100	5,000	5
3	RGB+Jet	1	–	–	0.1	100	100	5,000	5
4	RGB+Jet	1	–	–	1	100	100	5,000	5
5	RGB+Jet	1	–	–	10	100	100	5,000	5
6	RGB+Jet	1	–	–	100	100	100	5,000	5
7	RGB+Jet	1/2	–	–	1	0	100	5,000	5
8	RGB+Jet	1/2	–	–	10	100	100	5,000	5
9	Triple	1/2	1/2	6	–	–	300	15,000	15
10	Triple	1/2	1/2	12	–	–	300	15,000	15
11	Triple	2/3	1/3	6	–	–	300	15,000	15
12	Triple	1	10^{-3}	6	–	–	300	15,000	15
13	AGB	1	–	–	–	–	1500	75,000	75
14	AGB+Jet	1	–	–	1	0	500	25,000	25
15	AGB+Jet	1	–	–	1	500	500	25,000	25
Totals							4500	225,000	225
Test runs and convergence studies							500	25,000	–
Local storage									(125)
Total request							5000	**250,000**	**100**

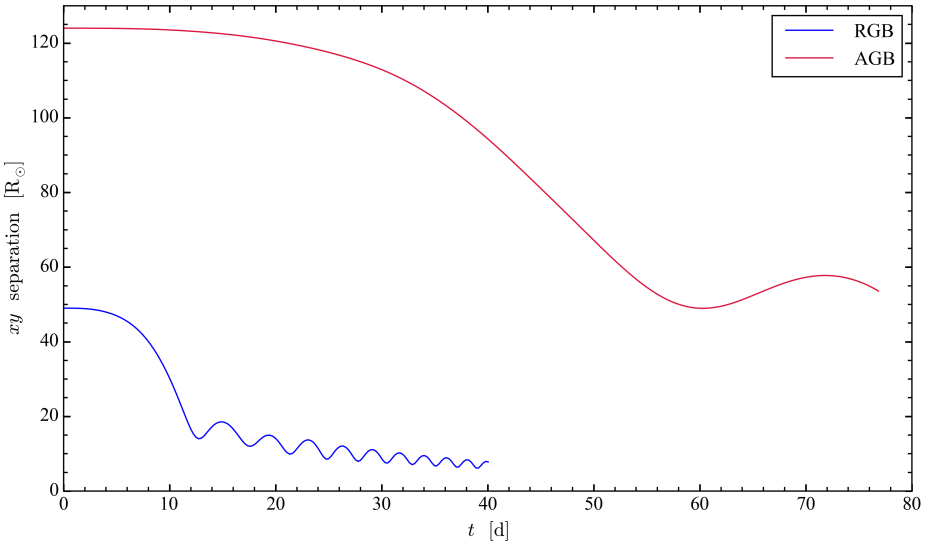

Figure 2: Inter-particle separation for the fiducial run (blue) and a test run with an AGB primary (red).

We have performed a low resolution trial run and the evolution of the orbital separation between the AGB core and secondary is shown in Fig. 2. The system must be evolved for about five times as long to reach the first periastron passage (first minimum of the curve). (The ratio of the dynamical time of the AGB star to that of the RGB star is about equal to the ratio of their radii to the 3/2 power by Kepler's third law, which is ~ 4. In practice this factor is ~ 5 because of the smaller gravitational drag on the secondary due to a more distended envelope.) This means that CEE simulations with an AGB primary evolve about five times slower than those with an RGB (for the same stellar masses). Since the number of AMR cells will be comparable, the AGB runs will require about five times more node-hours than the RGB runs.

The main AGB run will be performed in Run 13, which we will evolve for 300 d or 1500 frames. Although the evolutionary time scale is larger than in the RGB case, we choose to retain the same frame rate as it improves the fluidity of movies compared to that which could be attained in the fiducial run. We will perform two additional runs, Runs 14 and 15, that are similar to the jet runs 2 and 4, but now restarting from the AGB run, and lasting five times longer than those runs for the reason mentioned above.

5 Justification for SUs and TBs Requested

Our proposed runs are summarized in Tab. 1. Based on the scaling tests, we calculated in Sec. 3.3 that for a uniform frame rate of 5 frames per simulation day we require 50 node-hours per frame, based on 90% of frames computed with SKX nodes on Stampede 2, and 10% of frames computed on KNL nodes on Stampede 2. Multiplying the number of frames by the number of node-hours per frame, we arrive at the total number of node-hours per run, listed in the second-from-right column of Tab. 1. Summing the node-hours for each run, we arrive at the total 225,000 node-hours. We request an additional 25,000 node-hours for test runs and convergence studies. This brings the total requested value to **250,000 SUs** on Stampede 2. This is comprised of about 161,000 SUs on SKX nodes and 89,000 SUs on KNL nodes.

The mean storage requirement per frame for the fiducial run is about 50 GB as an hdf5 chombo file. This results in a total storage requirement of $\sim$ 225 TB. Our group has recently purchased a 120 TB Synology NSA diskstation, of which about 100 TB has been made available for storing simulation data from the proposed runs. In addition, about 25 TB can be stored relatively long-term on our local HPC resources. This leaves a shortfall of 100 TB. Therefore, we request a storage capicity of **100 TB** on TACC Ranch.

6 Additional Considerations

6.1 Research Team

Our research group consists of PI Professor Adam Frank, Co-PI Professor Eric Blackman, two computational scientists Baowei Liu and Jonathan Carroll-Nellenback, one post-doctoral computational astrophysicist Luke Chamandy, as well as two graduate students and one undergraduate student. The group has developed and maintained the AstroBEAR code, and applied it to many problems ranging from circumbinary disks to evolved star winds. Luke Chamandy and Baowei Liu will be running the proposed CEE simulations, with input from the other group members.

6.2 Local HPC Resources

The University of Rochester has two computational platforms available for our research. The Center of Integrated Research Computing (CIRC) hosts a Blue Gene/Q system called BlueStreak. BlueStreak consists of 1,024 nodes, 16 TB of RAM, and 400 TB of storage. Each node consists of a 16-core A2 processor with 32MB of cache and access to 16GB of RAM. CIRC also hosts a Linux cluster called BlueHive which has 284 nodes of IBM's iDataPlex architecture inter-connected with FDR10 Infiniband. Each BlueHive computing node houses 2X12-core Intel "Ivy Bridge" processors, with a range in memory from 64 GB to 512 GB. The entire BlueHive cluster has an InfiniBand-attached storage system providing $\approx$ 2PB of configurable raw disk within a GPFS file system. The Visualization nodes on BlueHive have OpenGL capable GPUs that can be used for accelerated 3D rendering. CIRC also hosts the Visualization-Innovation-Science-Technology-Application (VISTA) Collaboratory which is a state of the art visualization lab capable of displaying massive datasets in real time. VISTA is equipped with a 50 mega-pixel display and 10 Gbps direct fiber connection back to BlueHive and BlueStreak. These resources are available to researchers across the university and both systems are highly over-subscribed. Each user may use a maximum of 120 cores on BlueHive and we have used this resource for data analysis and, in some cases, for very low resolution tests of CEE runs. Our group has recently purchased a 120 TB Synology NSA diskstation.

6.3 Financial Support

We have been granted financial support from the NSF, DOE and NASA. Specifically the National Science Foundation, NSF AST-1813298 entitled "Interacting Binaries: Mass Transfer and Common Envelope Evolution" (PI, A. Frank; Co-PI, Eric Blackman 07/01/2018 - 06/30/2021); NSF AST-1515648 entitled "From Core to Outflow: The Dynamics of Binary Interactions and the Generation of Collimated Flows in Evolved Stars" (PI, A. Frank; 09/15/2015 - 08/31/2018); Space Telescope Sci Institute grant HST -AR-14563.02-A entitled "HST Cycle 24: Accretion to Outflow in Evolved Star Binaries: Disks in AGB, PPN and PN" (PI, A. Frank; 11/1/2016 - 10/31/2019) and DOE grant DE-SC0001063 entitled "From Interstellar Cloud to Star to Laboratory: Frontier HEDP Studies

of Magnetized Colliding Plasma Flows with Strong Radiative Cooling" (PI, A. Frank; 8/15/2015 - 8/14/2018).

7 Summary

We propose to run adaptive mesh refinement common envelope simulations on Stampede 2 at TACC using a combination of SKX and KNL nodes. For this purpose we request **250,000 SUs** on Stampede 2 (about 161,000 on SKX and 89,000 on KNL) and **100 TB** on TACC Ranch.

References

Balick B., Frank A., 2002, ARA&A, 40, 439

Carroll-Nellenback J. J., Shroyer B., Frank A., Ding C., 2013, Journal of Computational Physics, 236, 461

Chamandy L., Tu Y., Blackman E. G., Carroll-Nellenback J., Frank A., Liu B., Nordhaus J., 2018a, arXiv e-prints,

Chamandy L., et al., 2018b, MNRAS, 480, 1898

Chen Z., Frank A., Blackman E. G., Nordhaus J., 2016a, MNRAS, 457, 3219

Chen Z., Nordhaus J., Frank A., Blackman E. G., Balick B., 2016b, MNRAS, 460, 4182

Cunningham A., Frank A., Varnière P., Poludnenko A., Mitran S., Hartmann L., 2005, Ap&SS, 298, 317

Cunningham A. J., Frank A., Quillen A. C., Blackman E. G., 2006, ApJ, 653, 416

Cunningham A. J., Frank A., Varnière P., Mitran S., Jones T. W., 2009, ApJS, 182, 519

De Marco O., Izzard R. G., 2017, PASA, 34, e001

De Marco O., Passy J.-C., Frew D. J., Moe M., Jacoby G. H., 2013, MNRAS, 428, 2118

Duchêne G., Kraus A., 2013, ARA&A, 51, 269

Federrath C., Schrön M., Banerjee R., Klessen R. S., 2014, ApJ, 790, 128

Fogerty E., 2017, PhD thesis, University of Rochester

Fogerty E., Frank A., Heitsch F., Carroll-Nellenback J., Haig C., Adams M., 2016, MNRAS, 460, 2110

Gianninas A., Dufour P., Kilic M., Brown W. R., Bergeron P., Hermes J. J., 2014, ApJ, 794, 35

Grichener A., Sabach E., Soker N., 2018, MNRAS, 478, 1818

Günther M. N., et al., 2018, MNRAS, 478, 4720

Hansen E. C., Frank A., Hartigan P., Yirak K., 2015a, High Energy Density Physics, 17, 135

Hansen E. C., Frank A., Hartigan P., 2015b, ApJ, 800, 41

Hartigan P., et al., 2016, ApJ, 823, 148

Huarte-Espinosa M., Blackman E. G., Hubbard A., Frank A., 2013a, Mem. Soc. Astron. Ital., 84, 725

Huarte-Espinosa M., Carroll-Nellenback J., Nordhaus J., Frank A., Blackman E. G., 2013b, MNRAS, 433, 295

Iaconi R., Reichardt T., Staff J., De Marco O., Passy J.-C., Price D., Wurster J., Herwig F., 2017, MNRAS, 464, 4028

Ivanova N., 2018, ApJ, 858, L24

Ivanova N., et al., 2013, Astron. Astrophys. Rev., 21, 59

Jones D., Boffin H. M. J., 2017, Nature Astronomy, 1, 0117

Kaminski E., Frank A., Carroll J., Myers P., 2014, ApJ, 790, 70

Li S., Frank A., Blackman E. G., 2014, MNRAS, 444, 2884

Nandez J. L. A., Ivanova N., 2016, MNRAS, 460, 3992
Nordhaus J., Blackman E. G., 2006, MNRAS, 370, 2004
Ohlmann S. T., Röpke F. K., Pakmor R., Springel V., 2016, ApJ, 816, L9
Ohlmann S. T., Röpke F. K., Pakmor R., Springel V., 2017, A&A, 599, A5
Paczynski B., 1976, in Eggleton P., Mitton S., Whelan J., eds, IAU Symposium Vol. 73, Structure and Evolution of Close Binary Systems. p. 75
Paxton B., Bildsten L., Dotter A., Herwig F., Lesaffre P., Timmes F., 2011, ApJS, 192, 3
Paxton B., et al., 2013, ApJS, 208, 4
Paxton B., et al., 2015, ApJS, 220, 15
Poludnenko A. Y., Frank A., Mitran S., 2004, ApJ, 613, 387
Raghavan D., et al., 2010, ApJS, 190, 1
Reyes-Ruiz M., López J. A., 1999, ApJ, 524, 952
Sabach E., Hillel S., Schreier R., Soker N., 2017, MNRAS, 472, 4361
Shiber S., Soker N., 2018, MNRAS, 477, 2584
Soker N., 1994, MNRAS, 270, 774
Soker N., 2017, MNRAS, 471, 4839
Taam R. E., Sandquist E. L., 2000, ARA&A, 38, 113
Yirak K., Schroeder E., Frank A., Cunningham A. J., 2012, ApJ, 746, 133